INFLUENCE OF DIMENSION AND MAGNETIC INTERACTIONS ON ANNIHILATION AND NUCLEATION FIELDS OF PERMALLOY NANODISKS USING MICROMAGNETIC SIMULATIONS

INFLUENCIA DE LAS DIMENSIONES E INTERACCIONES MAGNÉTICAS EN LOS CAMPOS DE ANIQUILACIÓN Y NUCLEACIÓN DE NANODISCOS DE PERMALLOY USANDO SIMULACIÓN MICROMAGNÉTICA

Silvana R. Urcia-Romero,[1,2*] Helmunt E. Vigo-Cotrina[3] and Segundo R. Jáuregui-Rosas[1]

[1] Grupo Multidisciplinario de Investigación en Nanociencia y Nanotecnología, Departamento Académico de Física, Universidad Nacional de Trujillo, Trujillo, Perú.
[2] Department of Physics, University of Puerto Rico at Mayagüez, Mayagüez, Puerto Rico.
[3] Grupo de investigación en Ciencias Aplicadas y Nuevas Tecnologías, Universidad Privada del Norte, Trujillo, Perú.

(Recibido: Sep./2023. Aceptado: Dec./2023)

Abstract

Permalloy can exhibit magnetic vortex configurations depending on their dimensions and geometry, being of great interest due to potential applications in data storage and for cancer treatment. This work focuses on the effects of perpendicular uniaxial anisotropy, dimensions of permalloy nanodisks, and magnetostatic interactions on the annihilation and nucleation fields of magnetic vortices by means of micromagnetic simulations. Nanodisks with different diameters were evaluated, considering the effect of anisotropy generated by a platinum substrate for isolated nanodisks of 20 nm thickness. The effect of magnetostatic interactions for different arrays of identical nanodisks and a 10×10 array with random diameters from a normal distribution was also evaluated. The results show that

* silvana.urcia@upr.edu doi: https://doi.org./10.15446/mo.n68.110938

the annihilation and nucleation fields are influenced by the perpendicular uniaxial anisotropy. The higher the anisotropy, the more the annihilation field decreases, and the nucleation field increases, thus favoring the monodomain magnetic configuration. It was also shown that the magnetic interaction between the nanodisks and the lattice geometry led to a variation of the annihilation and nucleation fields. The magnetostatic interaction in the lattice leads to a collective rotation of the magnetic moments, so that the closing of the magnetic flux occurs randomly in a series of nanodisks minimizing the energy.

Keywords: Permalloy, nanodisk, micromagnetic simulation, magnetic vortex.

Resumen

Permalloy puede exhibir configuraciones de vórtices magnéticos dependiendo de sus dimensiones y geometría, siendo de gran interés debido a sus potenciales aplicaciones en el almacenamiento de datos y para el tratamiento del cáncer. Este trabajo se centra en los efectos de la anisotropía uniaxial perpendicular, las dimensiones de nanodiscos de aleación permalloy y las interacciones magnetostáticas sobre los campos de aniquilación y nucleación de vórtices magnéticos mediante simulaciones micromagnéticas. Se evaluaron nanodiscos con diferentes diámetros, considerando el efecto de la anisotropía generada por un sustrato de platino para nanodiscos aislados de 20 nm de espesor. También, se evaluó el efecto de las interacciones magnetostáticas para diferentes arreglos de nanodiscos idénticos y un arreglo de 10×10 con diámetros aleatorios con una distribución normal. Los resultados muestran que los campos de aniquilación y nucleación están influenciados por la anisotropía uniaxial perpendicular. Cuanto mayor es la anisotropía, más disminuye el campo de aniquilación y aumenta el campo de nucleación, favoreciendo así la configuración magnética monodominio. También se demostró que la interacción magnética entre los nanodiscos y la geometría de la red provocaba una variación de los campos de aniquilación y nucleación. La interacción

magnetostática en la red conduce a una rotación colectiva de los momentos magnéticos, de modo que el cierre del flujo magnético se produce de forma aleatoria en una serie de nanodiscos, minimizando la energía.

Palabras clave: Permaloy, nanodisco, simulación micromagnética, vórtice magnético.

Introduction

The magnetic configuration in ferromagnetic materials results from the competition of the different energies present, such as the exchange energy, the magnetostatic energy, and the anisotropy energy. Depending on factors such as geometry, size, and material, nanostructures can exhibit a magnetic configuration referred to as a magnetic vortex, where magnetic moments form a closed flow around a central point in this configuration [1–4]. Magnetic vortices have been observed using various experimental techniques, including electron microscopy and atomic force microscopy, among others [5–8]. Vortex magnetic moments can be oriented clockwise or counterclockwise. The circulation property of the magnetic vortex is defined as "c", with $c = +1$ for counterclockwise moments and $c = -1$ for clockwise. The magnetization at the central point of the vortex is perpendicular to the plane of the nanodisk and can point up or down. This defines the second vortex property, its polarity "p", where $p = +1$ is pointing up and $p = -1$ pointing down. Combining all the values of "c" and "p", it is possible to obtain four configurations for the magnetic vortex, $(c, p) = (1, 1), (1, -1), (-1, 1)$, and $(-1, -1)$, all of which have the same energy.

Nanostructures with vortices as their magnetic configuration have potential for a range of technological applications from data storage and spintronics [9–12] to magnetic sensors used in medicine for cancer treatment [13] to quantum information processing [14]. Using magnetic vortices in data storage presents specific benefits, such as allowing a high data storage density in a limited space, while the vortex stability can be advantageous for long-term storage

information. The capability of changing the vortex state in an efficient way contributes to the velocity of data reading and writing. In spintronics, the advantages of magnetic vortices are that they permit spin manipulations for data processing purposes and offer low energy dissipation. This, in turn, allows for the design of higher efficiency electronic devices with low energy consumption.

When a nanostructure is fabricated by the lithography method, the magnetic material is generally coupled to a substrate [15]. The latter can modify the magnetic properties of the material, inducing uniaxial anisotropy in the magnetic material. Anisotropy can alter the stability of the magnetic configuration established in the material, making it essential to study these effects that appear in real samples.

Iron-nickel alloys ($Ni_{80}Fe_{20}$), commonly known as Permalloy, exhibit remarkable magnetic response owing to their high Curie temperature, allowing them to withstand heat without affecting their properties [15, 16]. They are particularly notable for their high permeability, low coercivity, and significant anisotropic magnetoresistance, which contribute to magnetic stability. As previously mentioned, the stability of the magnetic properties at nanometer scales is also influenced by the size, shape, and of course type of the ferromagnetic material employed. Additionally, when this material is deposited on a heavy metal substrate (e.g., platinum), it is subject to an induced perpendicular uniaxial anisotropy.

Previous studies reported either on the influence of the perpendicular anisotropy or the magnetic interaction on the annihilation and nucleation fields. The former pertains to the magnetic field at which the transition from the magnetic vortex state to a monodomain state occurs, while the latter indicates the opposite [17, 18]. In the present work, we combine both effects, the perpendicular anisotropy, and the magnetic interaction, together with a size and shape effect to study their influence on the annihilation and nucleation fields.

Methodology

All the simulations were carried out using the free software MuMax3, which uses the finite differences method to numerically solve the Landau-Lifshitz-Gilbert (LLG) equation [19, 20].

$$\frac{\partial \vec{m}}{\partial t} = \frac{\gamma_{LL}}{1+\alpha^2}\left(\vec{m} \times \vec{B}_{eff} + \alpha\left(\vec{m} \times (\vec{m} \times B_{eff})\right)\right) \tag{1}$$

Where γ_{LL} is the gyromagnetic ratio (rad T/s), α is the damping constant (dimensionless), $\vec{B}_{\text{eff}}$ is the effective field (T), $\vec{m} = \vec{M}/M_s$ is the reduced magnetization (dimensionless), and M_s is the saturation magnetization (A/m).

In this study the effective magnetic field becomes:

$$\vec{B}_{\text{eff}} = \vec{B}_{\text{exchange}} + \vec{B}_{\text{magnetostatic}} + \vec{B}_{\text{anisotropy}} + \vec{B}_{\text{Zeeman}} \tag{2}$$

The terms denote respectively the contributions of the exchange, magnetostatic, anisotropic, and Zeeman fields.

The simulated universe was discretized in $5\,\text{nm} \times 5\,\text{nm} \times 5\,\text{nm}$ cells, and the main parameters considered are the exchange constant (A), the saturation magnetization (M_s), and the perpendicular uniaxial anisotropy constant (K_z). These values were chosen so that they correctly describe the material compared with experimental results for permalloy [21, 22]. The cell size was selected so that it is just smaller than the exchange length for permalloy (5.08 nm). For a larger cell size, the cell cannot be described by one effective magnetic moment, while smaller values increase the computational time without any appreciable changes to the annihilation and nucleation fields.

The parameter values used were the following: for the exchange constant $A = 13 \times 10^{-12}\,\text{J/m}$, the saturation magnetization $M_s = 860 \times 10^3\,\text{A/m}$, and the uniaxial anisotropy constant in the z-direction $K_z = 0, 100$, and $200\,\text{kJ/m}^3$ [23]. At higher values of

K_z, the vortex is destroyed, and the magnetic configuration of the nanodisk becomes a simple domain with moments oriented along the anisotropy axis.

1. Results and Discussion

The behavior of magnetization in permalloy nanodisks (with face-centered cubic structure) was studied, considering the effect of substrate-induced perpendicular uniaxial anisotropy, using micromagnetic simulations.

In the preliminary stage, simulations were conducted for different thicknesses ($t = 10\ and\ 20\ nm$) and diameters ($D = 100, 150, 300, 350, 450\ and\ 475\ nm$) to identify size ranges where the magnetic vortex configuration is the ground state. For this, an initial magnetic configuration with magnetic moments pointing in random directions was considered (Fig. 1(a)). The system was then allowed to relax until it reached the minimum energy condition $|\vec{m} \times \vec{B}_{\text{eff}}| < 10^{-5}$, which is achieved when a magnetic vortex forms in the nanodisk (Fig. 1(b)). Based on the results of the vortex ground state stability testing, we chose a thickness of 20 nm with diameters 300 nm and larger.

The hysteresis curves follow the conventional protocol and are obtained by applying a magnetic field B to a nanodisk (or an array of nanodisks) with a vortex magnetic configuration. This field is applied in the plane of the nanodisk and is gradually increased in intensity, in steps of $\Delta B_x = 0.1\,\text{mT}$, up to a maximum value of $100\ mT$, which is sufficient to saturate the sample. The values of the annihilation and nucleation fields were obtained from the maximum of the derivative dM/dB_x.

To analyze the effect of magnetic interactions between the nanodisks on the annihilation and nucleation fields of the vortex, various arrays were studied (see Fig. 3), such as monomers, trimers, squares, and a 10×10 matrix. In the latter, a Gaussian distribution with standard deviation $\sigma = 20$ was considered for the nanodisk diameters with fixed center-to-center separation ($d = 300\,\text{nm}$).

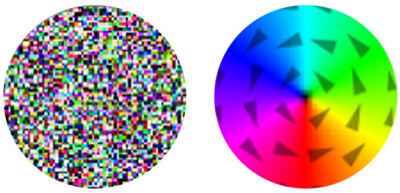

FIGURE 1. *(a) Representation of a random magnetic configuration, in (b) representation of the equilibrium vortex magnetic configuration, with circulation c = +1 and p = -1, obtained by micro-magnetic simulation for a 400 nm nanodisk with K_Z = 0 kJ/m^3*

1.1. Diameter and Uniaxial Anisotropy Effects on Isolated Nanodisks

Fig. 2 shows, on the left-hand side, a representative hysteresis curve for a 350 nm nanodisk, for $K_z = 0$. An external field B_x is applied to the nanodisk with a magnetic vortex configuration in the x direction until it is saturated. As can be seen, the magnetic moments that were initially circulating counterclockwise ($c = +1$) and with polarity ($p = -1$) (that is, they have a (1, -1) configuration) begin to progressively align in the direction of the applied field. As the applied field increases, the core of the vortex gradually moves in a direction perpendicular to the direction of the applied field until reaching a monodomain state, where the magnetic moments are completely aligned in the direction of the applied field.

The passage from the vortex state to the monodomain state occurs at a field, called the annihilation field, of $B_a = 75\,\mathrm{mT}$. By decreasing the value of the applied field, the nucleation field can be identified, which occurs at $B_n = 12\,\mathrm{mT}$, from which the magnetic moments once again form the vortex state. The vortex configuration is observed to change from (1, -1) to (-1, 1), which have the same energy. By gradually increasing the negative magnetic field, negative saturation is reached.

The right panel of Fig. 2 shows the evolution of a vortex in the presence of the applied magnetic field in the $+x$ direction. In (a), we have the configuration in the ground state, in (b), (c), and

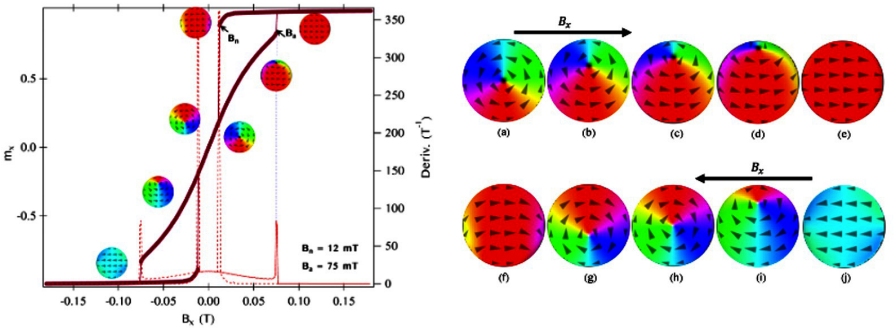

FIGURE 2. *Hysteresis loop (left panel) of an isolated nanodisk with $D = 350\,nm$ with $K_z = 0\,kJ/m^3$ and the evolution of the magnetic vortex (right panel) in the presence of an applied field in the $+x$ direction (upper right panel) and for a reversed magnetic field (lower right panel)*

(d), the evolution of the vortex is shown as the magnetic field increases, corresponding to the reversible movement of the nucleus. The nucleus moves in the $+y$ directions until it reaches saturation at (e). In (f), a reversed field is gradually applied until the formation of the vortex in (g), then follows the region where the magnetization responds linearly to the field and includes the remanent state without magnetization. The magnetic moments with the smallest deflection angle relative to the applied field ($+x$ direction) will align first, causing the nucleus to translate in the $+y$ direction until it finally vanishes from the nanodisk, annihilating the magnetic vortex configuration.

After annihilating the vortex, the magnetic moments will continue to orient themselves in the direction of the applied field until they all point in the same direction, forming a monodomain configuration. From (f), the intensity of the field is gradually reduced so that the magnetic moments stop pointing along the applied field and are ordered in such a way that, for a specific value of the magnetic field, the vortex appears again in the nanodisk (g). The value of this field is known as the nucleation field. Then, follows the region where the field intensity decreases to zero. In this region, the magnetic vortex is again in the equilibrium position (nucleus in the nanodisk center), corresponding to a remanent state without magnetization.

The exact process is applied, but in the opposite direction $(-x)$, where the magnetic behavior follows the path described above.

The same protocol to obtain the hysteresis curve is used for each of the evaluated nanodisks, finding that the annihilation field decreases by 12 % as the diameter of the nanodisk increases from 350 to 475 nm. In turn, the nucleation field reduces by 50 %, demonstrating the magnetostatic energy's dependence on the sample size. The larger the diameter of the nanodisk, the more unstable the vortex configuration. Therefore, the annihilation fields decrease, indicating a decrease in magnetostatic energy and an increase in the exchange interaction energy. This trend was also observed by Schneider et al. and Novosad et al., who reported that the annihilation fields depend on the nanodisk size and thickness; the smaller the diameter, the more significant the magnetostatic contribution [24, 25].

The annihilation fields evaluated in the presence of uniaxial anisotropy $K_z = 0, 100$, and $200\,\mathrm{kJ/m^3}$ decreased by 9.3 %, 4.2 %, 8.8 %, and 7.5 % for diameters of $350, 400, 450$, and 475 nm, respectively. Perpendicular anisotropy favors the alignment of the magnetic moments, decreasing their deviation from the direction of the applied field. On the other hand, the nucleation fields increase with the presence of anisotropy by 16.7 %, 14.4 %, 140 %, and 83 %, which is expected given that the higher the perpendicular uniaxial anisotropy, the configuration of the magnetic moments will be energetically favorable in the direction of the anisotropy, that is to say, that to obtain a vortex configuration they will have a higher energy cost with more significant anisotropy.

1.2. Magnetostatic Interaction and Perpendicular Uniaxial Anisotropy Influence on Different Arrays of Identical Nanodisks

Three different arrangements of identical nanodisks (dimer, trimer, and a 2×2 matrix), separated by an edge-to-edge distance of $d = 10, 50$, and 80 nm, were evaluated to analyze the effect of the magnetostatic interaction and the shape of the

array. The effect of uniaxial anisotropy was also evaluated with $K_Z = 0, 100,$ and $200\,\mathrm{kJ/m^3}$.

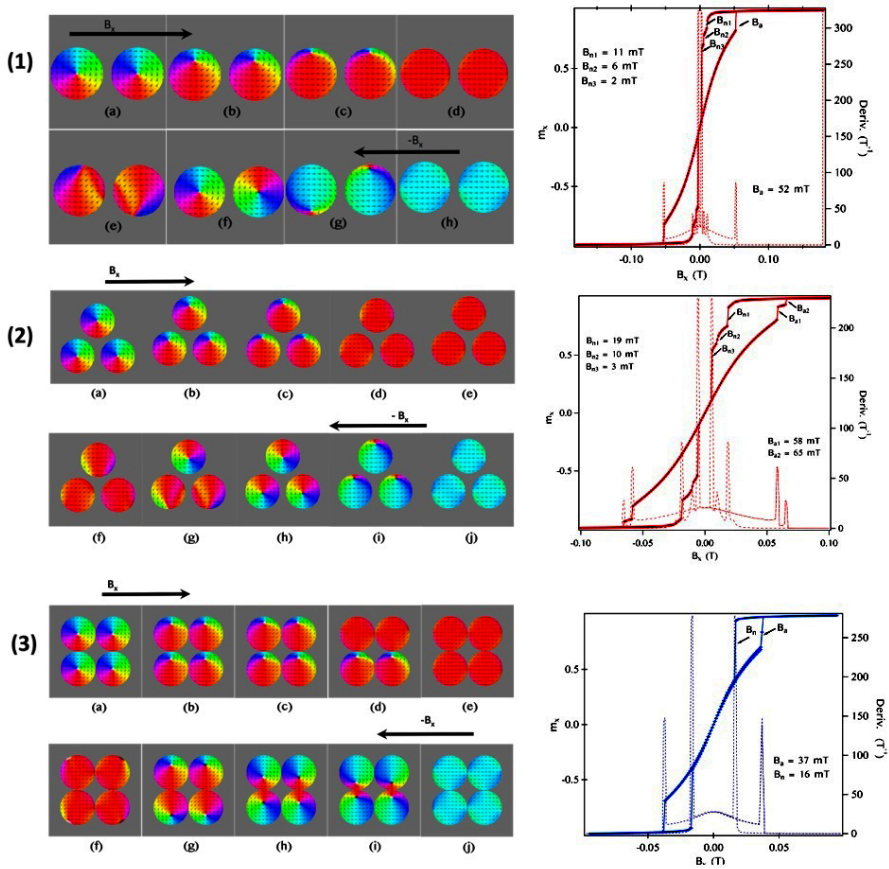

FIGURE 3. *Vortex evolution and hysteresis with its corresponding nucleation and annihilation fields of three identical nanodisk arrays: (1) Dimer with $D = 475\,nm$, $d = 80\,nm$, and $K_z = 0\,kJ/m^3$, (2) Trimer with $D = 400\,nm$, $d = 80\,nm$, and $K_z = 0\,kJ/m^3$, and (3) Square with $D = 475\,nm$, $d = 10\,nm$, and $K_z = 200\,kJ/m^3$*

Considering only the coupling effects in the three arrays evaluated (dimer, trimer, and the 2×2 matrix), it was found that the annihilation fields B_a increase with the increase in the separation distance between them, that is, at greater distances apart, the disks tend to behave like isolated disks due to the limited range of

magnetostatic interactions. In the presence of anisotropy ($K_z = 100$ and $200\,\mathrm{kJ/m^3}$), the annihilation fields B_a decrease monotonically as the anisotropy increases. The presence of the anisotropy causes a monotonic decrease in the annihilation fields, which ceases as soon as there is a competition between the magnetostatic interactions and the anisotropy. It is also shown that, when there are systems of two or more permalloy nanodisks, the transition of the annihilation and nucleation fields of the magnetic vortices do not occur simultaneously for a particular field value. That can happen progressively in each individual or two of the nanodisks (see Fig 3).

The presence of the magnetostatic interaction (when having a system of two or more identical nanodisks) plus the anisotropy would create an additional energy barrier for the transition from a single domain state to a vortex state, which generates an increase in the values of the nucleation fields. Therefore, it will favor the monodomain configuration in the direction of the applied field.

Fig. 3 shows in the left panel the evolution of a magnetic vortex for the three arrays evaluated. (1) For a dimeric arrangement with 475 nm diameter disks with $d = 80\,\mathrm{nm}$ and $K_z = 0\,\mathrm{kJ/m^3}$, in (2) for a trimeric system with 400 nm diameter nanodisks and $d = 80\,\mathrm{nm}$ and in (3) for a 2×2 matrix formed by disks with diameters of 475 nm at $d = 10\,\mathrm{nm}$ and $K_z = 200\,\mathrm{kJ/m^3}$. The respective hysteresis curves are presented on the right side of the graph.

Fig. 3-1 shows the vortex evolution as a function of the applied field. In (a), we have the vortex state, while in (b) and (c), it shows a translation of the core as the magnetic field gradually increases until it reaches the single domain. When there is a system of more than one nanodisk, an interaction between them will occur due to the uncompensated magnetic dipoles that appear on the surface, induced by the translation of the vortex nuclei. In Fig 3-2, as the magnetic field progressively increases, the cores of the vortices translate simultaneously. The nanodisks at the triangle's base are the first to pass to the single domain state, followed by saturation of the nanodisk at the top vertex. For the reversed field, nucleation occurs first in the nanodisk at the top vertex and then almost

simultaneously for the nanodisks at the base. As the negative field gradually increases, the evolution of the vortex and the transition to the monodomain state occur in a similar way described for the positive applied field. An arrangement of a 2×2 array of identical nanodisks with a diameter of 475 nm with a separation distance of 10 nm from edge to edge and $K_z = 200\,\mathrm{kJ/m^3}$ is shown in Fig 3-3. Starting from the vortex state (where all the nanodisks exhibit the same $p = +1$ polarity in (a), to show the process of transition from the vortex configuration in (b) to the single domain state in (e). The change to a single domain begins in the two nanodisks at the top of the lattice, see (d).

As the applied field decreases until reaching zero, the vortex nuclei in the first column of the array rotate in the $+y$ direction. In contrast, those nanodisks in the second column rotate in the opposite direction of $-y$. In (h), the vortices have reached equilibrium; the polarity of the vortices is alternating between $+1, -1$ and $-1, +1$ (which are energetically equal), respectively for each nanodisk. When the negative field is applied, the translation of the nuclei for the two nanodisks in the top row of the matrix is towards $-y$. However, for the two nanodisks in the bottom row this occurs towards the $+y$ direction until the vortex state disappears, giving rise to the single domain state.

Fig. 4 shows in (a) the annihilation and in (b) nucleation fields as a function of anisotropy. As can be seen, in nanodisk arrays, the annihilation and nucleation processes of the vortices occur over a range of fields. For example, for the arrangement of nanodisks with $K_z = 0\,\mathrm{kJ/m^3}$, the annihilation of the vortices in the system begins at $B_a = 68\,\mathrm{mT}$, achieving complete annihilation at $B_a = 78\,\mathrm{mT}$, this is also evidenced in Fig 5(a) which is visible as the steps present in the transition region. With anisotropy of $K_z = 200\,\mathrm{kJ/m^3}$ the range of annihilation fields decreases.

On the other hand, for the nucleation cases, the range of fields remains almost constant. The hysteresis curve for the transition region from monodomain to vortex state shows several steps. As shown in Fig. 5, the hysteresis for $K_z = 0$ exhibits a small coercivity,

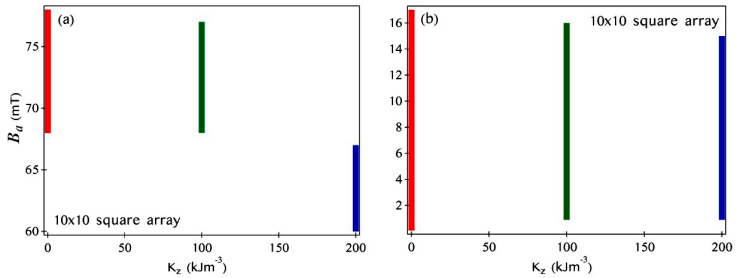

FIGURE 4. *In* (a)*, ranges of the annihilation fields* (B_a) *and in (b) nucleation fields* (B_n) *as a function of perpendicular uniaxial anisotropy for a square array of* 100 *nanodisks*

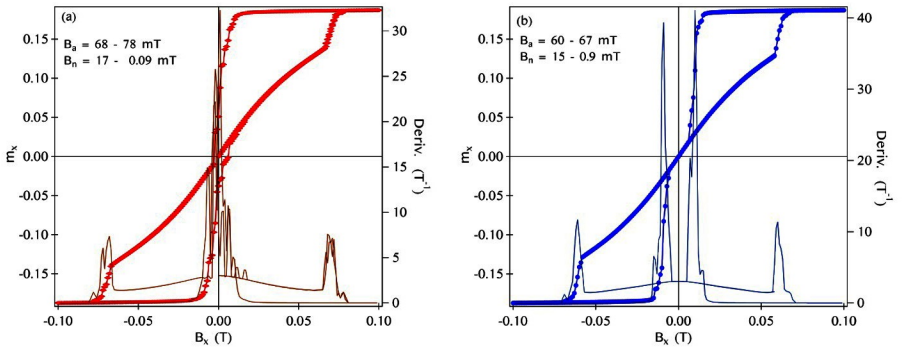

FIGURE 5. *Hysteresis loops for a* 10×10 *matrix in* (a) *absence of anisotropy and (b) with anisotropy* $K_z = 200\, kJ/m^3$

which is reduced for $K_z = 200\,\mathrm{kJ/m^3}$. Fig. 6 shows the annihilation mechanism for the 10×10 square lattice of nanodisks. In (a), the vortex state for the system is shown. In (b), the nuclei of the nanodisks move almost simultaneously towards the $+y$ direction, immediately after the annihilation process begins at a field of 68 mT. That starts with the nanodisks that are found in positions (6.5) and (7.5) within the matrix and continues then with those that are energetically favorable in passing to the monodomain state, in (c), (d), and (e).

Finally, the last ones to go to the monodomain state are those that are on the edge of the square lattice in (e), (f), (g), and (h), which will need more energy to be able to perform the transition.

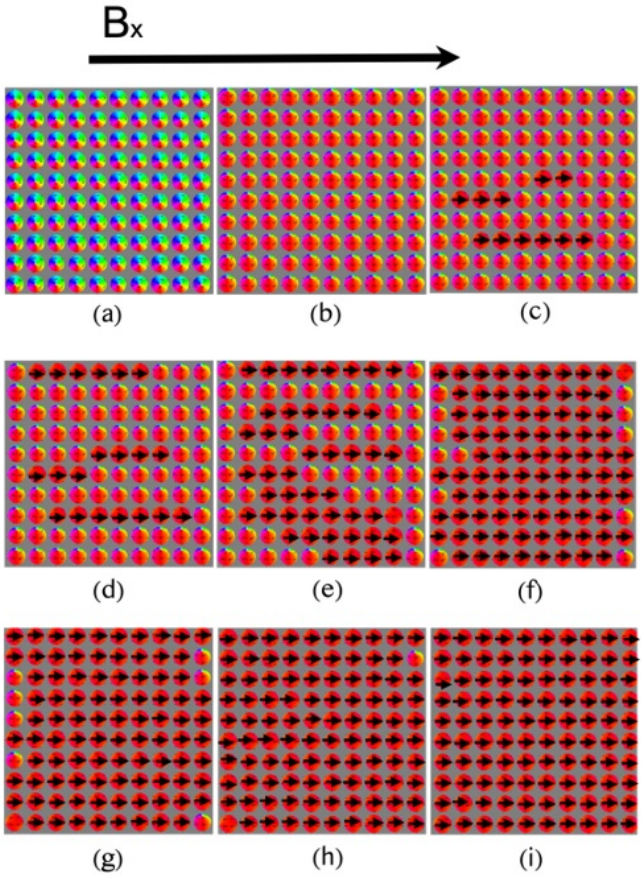

FIGURE 6. *Square arrays of* 100 *nanodisks under an applied magnetic field with* $K_z = 0$*; in (a) the array in vortex configuration and from (b) to (i) beginning of the vortex annihilation process until reaching saturation*

On the other hand, the nucleation process starts from the nanodisks located at the edges of the matrix, as shown in Fig. 7, from (a) to (d). Once the energetically favorable edge nanodisks nucleate, their nearest neighbors are subject to a reduced effective field compared to the nanodisks in the center. It can be seen in Fig. 7 (h), (i), (j), and (k) that nucleation occurs randomly. The magnetostatic interaction in the lattice leads to the collective rotation of the magnetic moments, so the magnetic flux closure can happen in a series of nanodisks to minimize the magnetostatic energy.

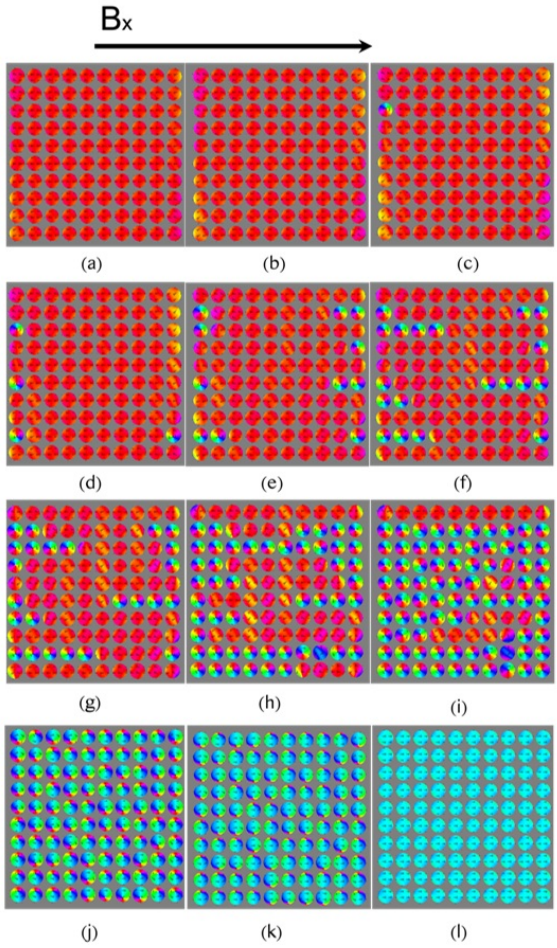

FIGURE 7. *Square lattice array of* 100 *nanodisks under an applied magnetic field with* $K_z = 0$*, in (a) lattice in monodomain configuration under the action of a magnetic field, the beginning of the vortex nucleation process in (c), and in (j), (k), and (l) negative magnetic field until reaching saturation*

Conclusions

The influence of perpendicular uniaxial anisotropy, nanodisk size, and magnetic coupling on the annihilation (B_a) and nucleation (B_n) fields of magnetic vortex configuration was studied using micromagnetic simulations. Simulations were performed for a dimer, a trimer, and a 2×2 matrix system, considering only identical

nanodisk arrays. A 10×10 square array system was also studied, in which the diameters of the nanodisks have a Gaussian distribution with $\bar{D} = 250\,\text{nm}$ with standard deviation $\sigma = 20$ and $t = 20\,\text{nm}$.

The results show that the magnetic vortex annihilation and nucleation field values are susceptible to perpendicular uniaxial anisotropy, leading to a decrease in annihilation field and an increase in nucleation field values when the anisotropy increases.

It was also shown that the effect of the magnetic interaction between the nanodisks and the array shape leads to a variation in the values of the B_a and B_n fields up to $\sim 73\,\%$. For nanodisks with large separations, the values for B_a and B_n tend to be those obtained as in the case of isolated nanodisks.

The results demonstrate the importance of considering the effects induced by the substrate and the magnetic interactions in this ferromagnetic material. In this case, the substrate induces perpendicular uniaxial anisotropy to the plane of the nanodisk, which can destabilize the vortex and therefore destroy it.

References

[1] R. V. Jain, L. Z. Tsai, and et al., J. Magn. Magn. Mater. **563**, 169901 (2022).

[2] Z. Zhang, J. Lim, and et al., J. Magn. Magn. Mater. **561**, 169727 (2022).

[3] D. Kuźma, L. Laskowski, and et al., J. Magn. Magn. Mater. **545**, 168685 (2022).

[4] A. Fernández, R. Streubel, and et al., Nat. Commun. **8**, 15756 (2017).

[5] N. Hirano, S. Kobayashi, and et al., Appl. Phys. Lett. **119**, 132401 (2021).

[6] P. Laha, B. Mahato, and et al., Appl. Phys. A **128**, 394 (2022).

[7] F. Guo, L. Belova, and R. McMichael, Phys. Rev. Lett. **110**, 017601 (2013).

[8] A. Vansteenkiste, K. Chou, and et al., Nature Phys. **5**, 332 (2009).

[9] W. Peng, L. Wang, and et al., J. Alloy. Compd. **910**, 164903 (2022).

[10] S. Piramanayagam and K. Srinivasan, J. Magn. Magn. Mater. **321**, 485 (2009).

[11] H. Zhang, H. Yu, and et al., Curr. Appl. Phys. **43**, 72 (2022).

[12] M. LoBue, F. Mazaleyrat, and et al., J. Magn. Magn. Mater. **322**, 1290 (2010).

[13] M. Ferreira, J. Sousa, and et al., Mater. **13**, 266 (2020).

[14] M. Martínez-Perez and D. Zueco, ACS Photonics **6**, 360 (2019).

[15] G. Nahrwold, J. Scholtyssek, and et al., J. Appl. Phys. **108**, 013907 (2010).

[16] K. Guslienko, V. Novosad, and et al., Appl. Phys. Lett. **78**, 3848 (2001).

[17] E. Novais, S. Allende, and et al., J. Appl. Phys. **114**, 153905 (2013).

[18] E. Novais, P. Landeros, and et al., J. Appl. Phys. **110**, 053917 (2011).

[19] A. Vansteenkiste, J. Leliaert, and et al., AIP Adv. **4**, 107133 (2014).

[20] L. Landau and E. Lifshitz, in *Perspectives in Theoretical Physics*, edited by L. Pitaevski (Pergamon, 1992) pp. 51–65.

[21] F. Garcia, J. Sinnecker, and et al., J. Appl. Phys. **112**, 113911 (2012).

[22] J. Sinnecker, H. Vigo, and et al., J. Appl. Phys. **115**, 203902 (2014).

[23] A. Guimarães, *Principles of Nanomagnetism*, NanoScience and Technology (Springer International Publishing, 2017).

[24] M. Schneider, H. Hoffmann, and et al., J. Appl. Phys. **92**, 1466 (2002).

[25] V. Novosad, K. Guslienko, and et al., Phys. Rev. B **65**, 060402 (2002).